



Electrochemical Immunosensor Based on Catalytic Activity of Nitrogen-doped Graphene Quantum Dots Supported by Graphene Nanoribbon Composite for Carbohydrate Antigen 15-3 Detection

Maryamosadat Mavaei^a, Ali Fattahi^{a,b,*} and Alireza Khoshroo^{a,*}

^aPharmaceutical Sciences Research Center, Health Technology Institute, Kermanshah University of Medical Sciences, Kermanshah, Iran

^bMedical Biology Research Center, Health Institute, Kermanshah University of Medical Sciences, Kermanshah, Iran

(Received 1 April 2021 Accepted 14 November 2021)

Due to the inherent properties of electrochemical immunosensors, they are widely considered to detect various biomarkers. This study developed an electrochemical immunosensor *via* the excellent catalytic effect of nitrogen-doped graphene quantum dot supported by graphene nanoribbon (N-GQD/GNR) composite as a sensing platform. Nafion was used as a binder for binding of N-GQD/GNR on the electrode surface. The modified electrode with N-GQD/GNR composite was applied to develop the label-free electrochemical immunosensor for the measurements of carbohydrate antigen 15-3 (CA15-3) biomarker. The catalytic activity of N-GQD/GNR nanocomposite increases the peak currents of the proposed immunosensor due to the accelerated electron transfer between the sensing platform and probe. This immunosensor has a wide linear range of 0.5–150.0 U ml⁻¹, with a detection limit of 0.1 U ml⁻¹. Also, the proposed immunosensor has significant specificity, high sensitivity, and accuracy. The prepared electrochemical immunosensor was used to detect CA15-3 protein in blood samples.

Keywords: Graphene nanoribbons, N-doped-Graphene quantum dots, Electrochemical immunosensor, Carbohydrate antigen 15-3

INTRODUCTION

The electrochemical sensors based on carbon-based materials exhibit excellent characteristics due to their unique chemical and physical properties, such as high electrocatalytic activity and interfacial adsorption properties [1]. The electrocatalytic properties can be further improved through surface modification with various nanostructured materials with synergistic properties [2–7]. Among carbon-based materials, graphene (GR) has been widely used in different electrochemical assays such as sensors [8,9], fuel cells [10], and supercapacitors [11]. Recently, graphene nanoribbons (GNR) have emerged as a one-dimensional material with a sizeable bandgap for different applications.

Graphene quantum dots (GQD) appears to be a good candidate for the functionalization of GNR due to their excellent characteristics including multiple active edges and catalytic properties [12,13]. Joseph W. Lyding *et al.* [14] have investigated the influence of edge defects on the electronic properties of GQD and GNR with tunneling spectroscopy. In another work, Jichang Wang *et al.* have reported that GQD supported by GNR with edge defects on the composite surfaces showed excellent catalytic activities for oxygen reduction (higher performance than pt). The presence of heteroatoms in carbon-based material structures can effectively change the electronic characteristics. The nitrogen atom with 5 valence electrons has been extensively applied for doping in carbon-based material [15,16]. Doping of nitrogen in graphene quantum dots (N-GQD) provides further edge active sites, high surface area, and superior crystal structure [17,18]. Gervasio *et al.* [19] found that

*Corresponding authors. E-mail: Khoshroo.a.r@gmail.com; a.fattahi.a@gmail.com

doping nitrogen in graphene quantum dots increased the electrochemical activity toward 2,4,6-trinitrotoluene reduction. Several nanocomposite materials based on the GNR for sensor modification were introduced such as poly(diallyl dimethylammonium chloride)/gold nanoparticle [20], polyaniline nanorods grown on GNR [21], GNR/polypyrrole [22], GNR/Co coordination polymer nanohybrids [23], PtPd/GNR alloy [24] and PdNi nanoparticles, and N-doped GNR [25].

CA15-3 is one of the major breast cancer biomarkers used in monitoring therapy outcomes and disease progression in metastatic breast cancer patients [26]. The normal concentration of CA15-3 is under 30 U ml⁻¹ in blood. When the CA15-3 concentrations exceed 100 U ml⁻¹, it can be considered as a disease [27]. The level of CA15-3 could provide valuable details to record the 'patients' postoperative condition, and it can also predict recurrence and metastasis of tumor. Therefore, detecting CA15-3 biomarkers is very valuable because it helps in the diagnosis of cancer at early stages and/or the prognosis of the patient in therapy programs [28]. Electrochemical immunosensor has an excellent benefit for diagnosing CA15-3 due to its properties, *i.e.*, high sensitivity, portability, inexpensive and easy miniaturization.

This study developed a composite material based on GNR with heteroatom doped GQD (N-GQD/GNR) to construct an electrochemical immunosensor for CA15-3 determination. The N-GQD/GNR composite provides an outstanding platform for immobilization antibodies to detect CA15-3 protein in serum samples.

EXPERIMENTAL

Reagents and Apparatus

CA15-3 antibody and CA15-3 antigen are from Abcam (United Kingdom). Multi-walled carbon nanotubes (MWCNTs), potassium permanganate, citric acid monohydrate, Nafion (NF), uric acid, phosphate salt, potassium chloride, hydrochloric acid, ether, dimethylformamide (DMF), graphite, solvents, and other reagents are from Merck (Darmstadt, Germany).

Electrochemical investigations were performed in a three-electrode cell with an Autolab PGSTAT101 system (Eco Chemie, Netherlands). The morphology of the

nanocomposites was studied by SEM (TESCAN, Czech Republic). The composite powder was dispersed in DMF/water, sonicated for 30 min, and then drop cast the composite dispersion on double-sided adhesive tape glued to one end of the SEM sample holder. The N-GQD/GNR-Au composite modified glassy carbon electrode (N-GQD/GNR-Au/GCE) was used as a working electrode.

Preparation of N-GQD

The nitrogen-doped graphene quantum dot was synthesized with a hydrothermal method. The urea and citric acid were used as nitrogen and carbon sources, respectively. The urea (0.18 g) and citric acid (0.21 g) were dissolved in 5 ml deionized (DI) water, and the solution was heated at 160 °C in the Teflon-lined autoclave for 4 h. Then, the autoclave was cooled to room temperature (RT). Finally, the upper aqueous solution was collected by centrifugation [29].

Preparation of GNR and N-GQD/GNR

MWCNTs (0.1 g) were dispersed in sulfuric acid (10 ml), and KNO₃ (1.0 g) was added to the above mixture and stirred (300 rpm) for 120 min. Then, KMnO₄ (0.5 g) was added to the above mixture and stirred for 120 min. Subsequently, the mixture was heated at 70 °C for 120 min in a water bath and cooled to RT. Next, the ice (350 g) containing H₂O₂ (5.0 ml) was added to the obtained mixture. The GNR was collected by centrifugation and was ultrasonically dispersed in DI (60 ml), and HCl (30 ml) was added to the mixture. The precipitate was centrifuged and then ultrasonically dispersed in ether (60 ml). Finally, GNR was collected by centrifugation and dried at 70 °C for overnight [30].

In the synthesis of N-GQD/GNR, GNR aqueous dispersion (4.0 ml, 2 mg ml⁻¹) and N-GQD (2.0 ml, 1.5 mg ml⁻¹) were dispersed in 10.4 ml DI water in an ultrasound bath for 20 min. The suspension was heated at 180 °C in the Teflon-lined autoclave for 12 h. The precipitate was collected by centrifugation and washed with DI water.

Preparation of Electrochemical Immunosensor

The modification of glassy carbon electrode (GCE)

with N-GQD/GNR-Au composite is described as follows; 2 mg N-GQD/GNR and 30 μ l nafion were dispersed in 1.0 ml DMF/water (ratio 1:1) in an ultrasound bath for 30 min. Nafion was used as a binder for binding of N-GQD/GNR on the electrode surface. After cleaning GCE with alumina, 2 μ l of the nanocomposite was applied on the GCE and dried at RT (N-GQD/GNR/GCE). Then, Gold NPs were deposited on N-GQD/GNR/GCE via electrodeposition in HAuCl₄ (1.2 mM) and H₂SO₄ (0.5 mM). The electrodeposition was carried out by 5 cycles of cyclic voltammetry (CV) method in the range of -0.5 to +1.2 V and scan rate of 100 mV s⁻¹ (N-GQD/GNR-Au/GCE).

Subsequently, 7 μ l of antibody (50 ppm) was cast on N-GQD/GNR-Au/GCE for 60 min and then washed with buffer solution. Then, 7 μ l of cysteine (1.0 mM) was placed on the surface for 60 min to cover the sites between antibodies. The immunosensor (designed as N-GQD/GNR-Au-Ab/GCE) was used to detect the CA15-3 antigen.

Measurement Procedure

The prepared immunosensor (N-GQD/GNR-Au/Ab/GCE) was immobilized with various amounts of CA15-3 antigen for 180 min, and then the electrode was rinsed with buffer solution. The electrochemical signals were obtained in the presence of 1.0 mM catechol. The formation of CA15-3 antigen-antibody complexes has blocked the surface of N-GQD/GNR-Au toward the oxidation of catechol. Therefore, the differential pulse voltammetry (DPV) signals decreased in the presence of antigen. These signal changes are proportional to the concentration of antigen, which is applied to measurements of CA15-3 antigen. Figure 1 shows the fabrication procedure of N-GQD/GNR-Au/Ab/GCE.

RESULTS AND DISCUSSION

Characterization of the Materials

The raw untreated multi-walled carbon nanotubes (MWCNTs) show characteristic tubular structures [31]. In this work, the tubular structures of MWCNTs were open by introducing KMnO₄. The SEM of GNR showed ribbon morphology that is formed from unzipped external walls of MWCNTs (Figs. 2A and B). The change of the tubular structure of MWCNTs to nanoribbons indicates the

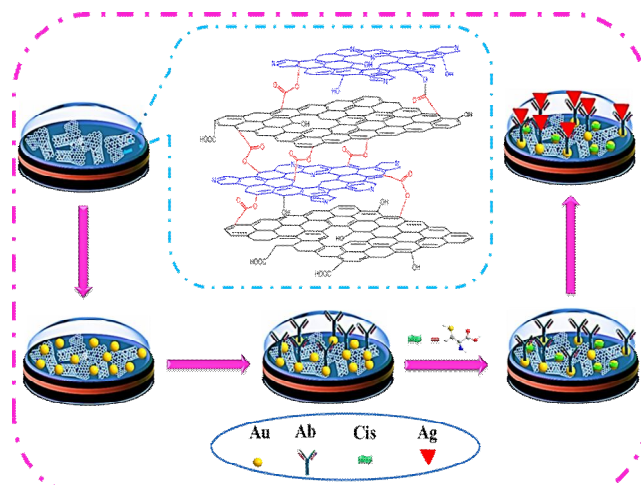


Fig. 1. Schematic exhibition of the fabrication process of the immunosensor

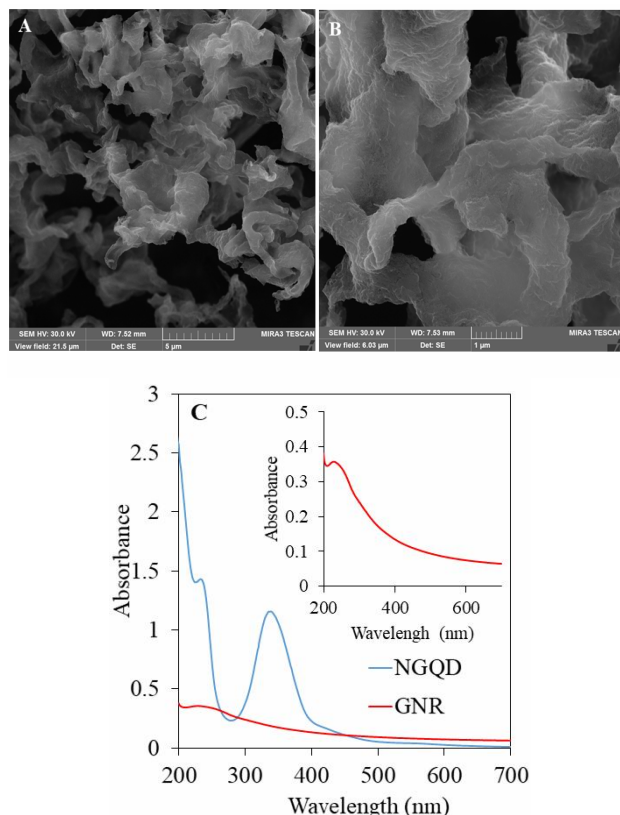


Fig. 2. (A) and (B) SEM of N-GQD/GNR at different magnifications, (C) UV-Vis spectrum of the NGQD and GNR. Inset shows the magnification of the spectrum of GNR.

successful unzipping of MWCNTs. Figure 2C shows the UV-Vis spectrum of NGQD and GNR. A distinctive adsorption peak at 240 nm, relative to the $\pi-\pi^*$ transition of the aromatic ring, was observed. The absorption peak at 340 nm is relative to the $n-\pi^*$ transition of carbon and nitrogen [32], confirming N doping formation in GQD [33]. These results confirm the unzipping process of MWCNTs.

The catalytic effect and stepwise fabrication of GNR/N-GQD-Au/GCE were studied with electrochemical impedance spectroscopy (EIS), and CV. Figure 3A shows the Nyquist plots for GNR/GCE (a), GNR/N-GQD/GCE (b), and GNR/N-GQD/Au/GCE (c) in 2.0 mM $[Fe(CN)_6]^{3+/4+}$. The charge transfer resistance (R_{ct}) was decreased by adding GNR, N-GQD, and Au to the GCE, GNR/GCE, and the GNR/N-GQD/GCE. Therefore, the presence of GNR, N-GQD, and Au on composite effectively increased the electron transfer on the sensor. These results show the successful formation of GNR/N-GQD/Au on the GCE.

The effect of the GNR/N-GQD/Au composite on catalytic currents was studied by CV in the presence of 2.0 mM catechol (PBS, pH = 7.4). Figure 3B shows the CVs of GNR/GCE (a), GNR/N-GQD/GCE (b), and GNR/N-GQD/Au/GCE (c) in the range of -0.15 to 0.6 V (Fig. 3B) at the scan rate of 100 mV⁻¹. All modified electrodes show a pair of redox peaks for the oxidation of catechol to its quinone and reduce the quinone back to catechol. As shown in Fig. 3B, after the addition of N-GQD (GNR/N-GQD/GCE, curve b) and AuNPs (GNR/N-GQD/Au/GCE, curve c) to GNR (GNR/GCE, curve a), the peak current increased due to the catalytic effect and high specific surface area of GNR/N-GQD/Au composite. The increase of the CV currents during the stepwise fabrication of GNR/N-GQD/Au on the electrode is another evidence of GNR/N-GQD/Au/GCE formation.

The CVs of the GNR/N-GQD/Au/GCE were studied at various pH values. Figure 4A shows the GNR/N-GQD/Au/GCE CVs in the presence of 1.0 mM catechol at different pH values ranging from 4.0 to 8.0. The peak potential of catechol was pH-dependent (Fig. 4B). The results show that the slope of anodic and cathodic peak potential vs. pH are -58.1 and -55.3 mV/pH, respectively. This slope was close to the Nernstian value of -59.2 mV for a two-electron, two-proton process [34]. Furthermore, GNR/N-GQD/Au/GCE shows much higher peak currents

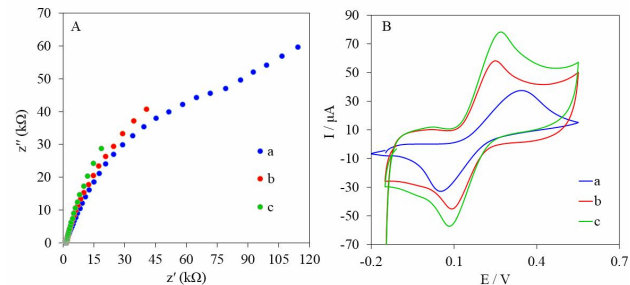


Fig. 3. (A) EIS of GNR/GCE (a), GNR/N-GQD/GCE (b) and GNR/N-GQD/Au/GCE (c) in 0.1 M KCl and 2.0 mM $[Fe(CN)_6]^{3+/4+}$ (B) CVs of GNR/GCE(a), GNR/N-GQD/GCE (b) and GNR/N-GQD/Au/GCE (c) in 0.1 M PBS (pH = 7.4) containing 2.0 mM catechol.

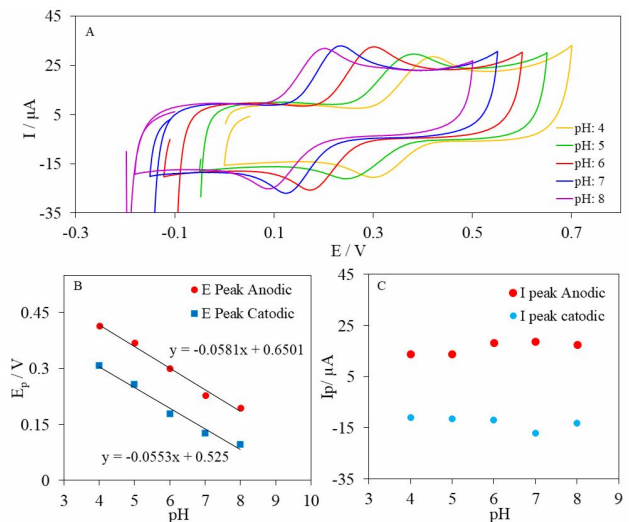


Fig. 4. (A) CVs of GNR/N-GQD/Au/GCE in the presence of 1.0 mM catechol and 0.1 M PBS with different pHs, from 4 to 8 containing. Variation of E_p (B) and I_p (C) vs. pH.

toward catechol in the pH = 7 (Fig. 4C); therefore, this pH was used as optimum one for subsequent experiments.

Electrochemical Behavior of Engineered Immunosensor

The interaction of immobilized antibody on GNR/N-

GQD/Au/Ab/GCE with CA15-3 antigen was investigated with EIS, and CV. Figure 5 shows the EIS (Fig. 5A) spectra and CVs (Fig. 5B) of GNR/N-GQD/Au/GCE (curve a), GNR/N-GQD/Au/Ab/GCE (curve b) and GNR/N-GQD /Au/Ab/Ag/GCE (curve c). As can be seen, after immobilization of anti-CA15-3 on the GNR/N-GQD /Au/GCE surface, semicircle diameter of EIS spectra was increased (curve b, Fig. 5A) and the peak current was decreased (curve b, Fig. 5B), which suggested that the immobilization of anti-CA15-3 as blocking layers on the electrode and disturbs the electron transfer between the catechol in solution and the GNR/N-GQD /Au/GCE.

After the GNR/N-GQD/Au/Ab captured CA15-3 antigen, there is another increase in semicircle diameter (R_{ct}) (curve c, Fig. 5A) and decrease of the CV currents (curve c, Fig. 5B), suggesting an interaction between the antibody and CA15-3 antigen on the sensing platform, which acts as an insulating layer of protein and hindered the electron transfer between the catechol and GNR/N-GQD/Au. These results also confirm an efficient bonding of CA15-3 antigen on the GNR/N-GQD/Au/Ab surface.

Optimization of Detection Conditions

Various parameters, e.g., CA15-3 antibody concentration and immobilization time on the electrode surface and incubation time of antigen, were evaluated to achieve the best response to the CA15-3 antigen. As illustrated in Fig. 6, by increasing the immobilization time of CA15-3 antibody from 30 to 240 min at the GNR/N-GQD/Au/GCE, the current decreased and reached a minimum value at 60 min and then increased (Fig. 6A); therefore, 60 min was selected as the optimum time for incubation of CA15-3 antibody. Furthermore, the amount of CA15-3 antibody on the GNR/N-GQD/Au/GCE from 25 to 100 ppm was also investigated (Fig. 6B). Based on the obtained results, 50 ppm was chosen as the optimum amount of CA15-3 antibody. The effect of the immobilization times of CA15-3 antigen on the signal of GNR/N-GQD/Au/Ab/GCE was evaluated, and a time of 3 h was selected (Fig. 6C).

Analytical Approach

The linear range and limit of detection (LOD) of GNR/N-GQD/Au/Ab/GCE toward CA15-3 antigen

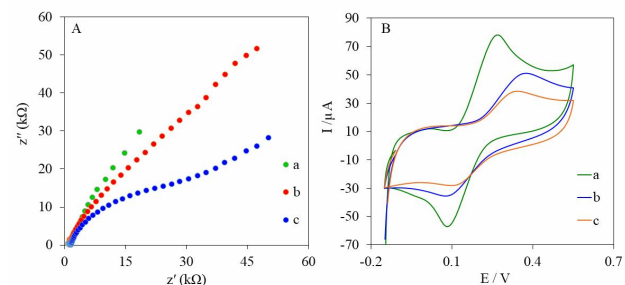


Fig. 5. (A) EIS of GNR/N-GQD/Au/GCE (a), GNR/N-GQD/Au/Ab/GCE (b) and GNR/N-GQD/Au/Ab/Ag/GCE (c) in 0.1 M KCl and 2.0 mM $[\text{Fe}(\text{CN})_6]^{3-/4-}$ (B) cyclic voltammograms of GNR/N-GQDAu/GCE (a), GNR/N-GQD/Au/Ab/GCE (b) and GNR/N-GQD/Au/Ab/Ag/GCE (c) in 0.1 M PBS (pH = 7.4) containing 2.0 mM catechol.

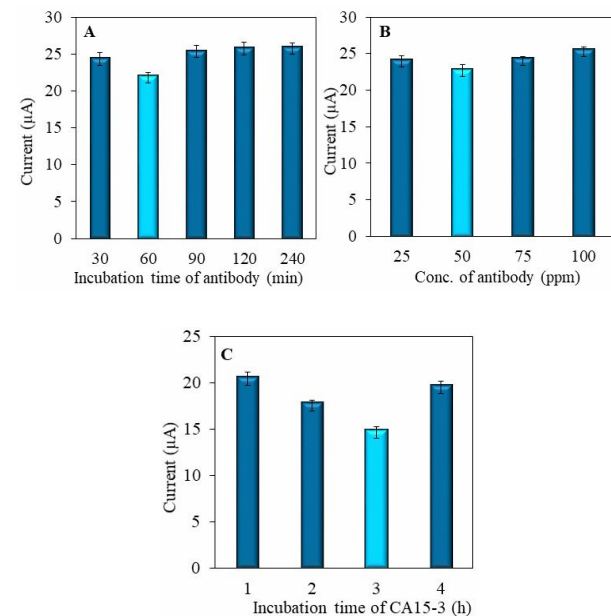


Fig. 6. Optimization of: (A) incubation time of anti-CA15-3 and (B) the concentration of anti-CA15-3, (C) incubation time of CA15-3 antigen.

were evaluated by measurements of various protein concentrations by differential pulse voltammetry in the presence of 2.0 mM catechol. The DPV signals decreased with increased CA15-3 antigen due to the blocking of the

Table 1. A Comparison with other Sensors for the Detection of CA15-3

Detection methods	Linear range (U ml ⁻¹)	Detection limit (U ml ⁻¹)	Ref.
Label-Free Fluorescent Aptasensor	10-500	10	[35]
Quartz crystal microbalance	0.5-26	-	[36]
Surface plasmon resonance	1-40	0.025	[37]
Electrochemiluminescence	0.05-120	0.014	[38]
Scanning electrochemical microscopy	15-250	2.5	[39]
Enzyme-free electrochemical immunosensor	0.1-150	0.03	[40]
The kinetic-exclusion analytical technology	0.3-20	0.21	[41]
Optical sensing	1.25-25	0.4	[42]
Enzyme-linked immunosensor	0.1-160	0.04	[43]
GNR/N-GQD/Au/Ab/GCE	0.5-150	0.1	This work

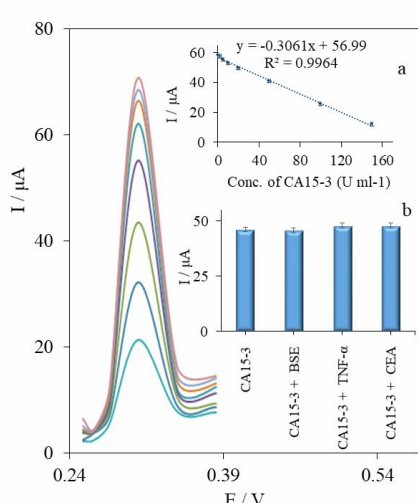


Fig. 7. DPV responses of the immunosensor to 2.0 mM catechol in phosphate buffer (pH = 7.4) at different concentrations of CA15-3 antigen. The numbers of 1-8 correspond to: 150.0, 100.0, 50.0, 20.0, 10.0, 5.0, 2.0, and 0.5 U ml⁻¹, respectively. The inset is the calibration curve. DPV was performed with an amplitude of 0.05 V, a pulse width of 0.2 s, a sampling width of 0.05 s, and a pulse period of 0.5 s.

electron transfer on the GNR/N-GQD/Au/Ab/GCE (Fig. 7). The proposed assay showed an acceptable linear range from 0.5 to 150.0 U ml⁻¹. The LOD for the GNR/N-

GQD/Au/Ab/GCE was 0.1 U ml⁻¹ (S/N of 3σ). The selectivity of the GNR/N-GQD/Au/Ab toward CA15-3 antigen was an investigation in the presence of BSA, CEA, and TNF-α. The results were presented in Fig. 7 (inset b), suggesting that the presence of the interfering species causes minimum changes in the GNR/N-GQD/Au/Ab responses toward CA15-3 antigen. The analytical performance of the GNR/N-GQD/Au/Ab was compared with some published data for CA15-3 antigen sensors in Table 1.

Reproducibility and Stability

GNR/N-GQD/Au/Ab/GCE's reproducibility was investigated with immunosensor prepared with the same procedure and applied to the same amount of antigen. The RSD of six GNR/N-GQD/Au/Ab/GCE toward determination of the 20 U ml⁻¹ and 5 U ml⁻¹ of antigen were 1.32% and 2.09%, respectively, indicating the proposed sensor's good reproducibility. GNR/N-GQD/Au/Ab/GCE's stability is determined after storing immunosensors at 4 °C in the refrigerator. Based on the obtained results, after 35 days, the signal of the immunosensor was about 91% of its initial signal, which suggested that the GNR/N-GQD/Au/Ab/GCE had good stability.

CONCLUSIONS

A sensitive method was introduced to detect CA15-3 antigen based on GNR/N-GQD/Au nanocomposites as

the efficient material for electrode modification. This nanocomposite shows good catalytic properties toward the oxidation of catechol and provided a high surface area for immobilization of CA15-3 antibody as recognition elements for measurements of CA15-3 antigen. The electrode modified with GNR/N-GQD/Au nanocomposite presented some advantages, including enzyme-free method, wide linear range measurements, simple method, and good reproducibility, which could provide a reliable way for analysis of CA15-3 antigen.

ACKNOWLEDGMENTS

The authors gratefully acknowledge the Research Council of Kermanshah University of Medical Sciences for financial support.

REFERENCES

- [1] Z. Wang, J. Yu, R. Gui, H. Jin, Y. Xia, *Biosens. Bioelectron.* 79 (2016) 136.
- [2] M. Mazloum-Ardakani, L. Hosseinzadeh, A. Khoshroo, *Electroanalysis* 27 (2015) 2518.
- [3] M. Mazloum-Ardakani, S.H. Ahmadi, Z.S. Mahmoudabadi, A. Khoshroo, *Measurement* 91 (2016) 162.
- [4] R. Kour, S. Arya, S.-J. Young, V. Gupta, P. Bandhoria, A. Khosla, *J. Electrochem. Soc.* 167 (2020) 37555.
- [5] M.H. Ghanbari, F. Shahdost-Fard, M. Rostami, A. Khoshroo, A. Sobhani-Nasab, N. Gholipour, H. Salehzadeh, M.R. Ganjali, M. Rahimi-Nasrabadi, F. Ahmadi, *Microchim. Acta* 186 (2019) 698.
- [6] A. Khoshroo, K. Sadrjavadi, M. Taran, A. Fattahi, *Sensors Actuators B Chem.* 325 (2020) 128778.
- [7] A. Khoshroo, A. Fattahi, *Sci. Rep.* 10 (2020) 1.
- [8] A. Khoshroo, L. Hosseinzadeh, K. Adib, M. Rahimi-Nasrabadi, F. Ahmadi, *Anal. Chim. Acta* 1146 (2021) 1.
- [9] M. Mazloum-Ardakani, M. Zokaie, A. Khoshroo, *Ionics (Kiel)*. 21 (2015) 1741.
- [10] E. Antolini, *Appl. Catal. B Environ.* 123 (2012) 52.
- [11] J.J. Yoo, K. Balakrishnan, J. Huang, V. Meunier, B.G. Sumpter, A. Srivastava, M. Conway, A.L. Mohana Reddy, J. Yu, R. Vajtai, *Nano Lett.* 11 (2011) 1423.
- [12] X.T. Zheng, A. Ananthanarayanan, K.Q. Luo, P. Chen, *Small* 11 (2015) 1620.
- [13] H. Kooshki, A. Sobhani-Nasab, M. Eghbali-Arani, F. Ahmadi, V. Ameri, M. Rahimi-Nasrabadi, *Sep. Purif. Technol.* 211 (2019) 873.
- [14] K.A. Ritter, J.W. Lyding, *Nat. Mater.* 8 (2009) 235.
- [15] D. Guo, R. Shibuya, C. Akiba, S. Saji, T. Kondo, J. Nakamura, *Science (80-)* 351 (2016) 361.
- [16] E. Sohouli, F. Shahdost-Fard, M. Rahimi-Nasrabadi, M.E. Plonska-Brzezinska, F. Ahmadi, *J. Electroanal. Chem.* 871 (2020) 114309.
- [17] J. Huang, J. Han, T. Gao, X. Zhang, J. Li, Z. Li, P. Xu, B. Song, *Carbon N. Y.* 124 (2017) 34.
- [18] S.S. Yu, W.T. Zheng, Q.B. Wen, Q. Jiang, *Carbon N. Y.* 46 (2008) 537.
- [19] Z. Cai, F. Li, P. Wu, L. Ji, H. Zhang, C. Cai, D.F. Gervasio, *Anal. Chem.* 87 (2015) 11803.
- [20] Y. Yao, K. Shiu, *Electroanal. An Int. J. Devoted to Fundam. Pract. Asp. Electroanal.* 20 (2008) 1542.
- [21] L. Li, A.-R.O. Raji, H. Fei, Y. Yang, E.L.G. Samuel, J.M. Tour, *ACS Appl. Mater. Interfaces* 5 (2013) 6622.
- [22] F.-H. Hsu, J.-W. Huang, T.-M. Wu, *Mater. Chem. Phys.* 161 (2015) 265.
- [23] S.K. Ujjain, P. Ahuja, R.K. Sharma, *J. Mater. Chem. B* 3 (2015) 7614.
- [24] Y. Liu, L. Wei, Y. Hu, X. Huang, J. Wang, J. Li, X. Hu, N. Zhuang, *J. Alloys Compd.* 656 (2016) 452.
- [25] N. Li, H. Ma, W. Cao, D. Wu, T. Yan, B. Du, Q. Wei, *Biosens. Bioelectron.* 74 (2015) 786.
- [26] J.A. Koepke, *Cancer* 69 (1992) 1578.
- [27] J. Wu, Z. Fu, F. Yan, H. Ju, *TrAC Trends Anal. Chem.* 26 (2007) 679.
- [28] H. Alexander, A.L. Stegner, C. Wagner-Mann, G.C. Du Bois, S. Alexander, E.R. Sauter, *Clin. Cancer Res.* 10 (2004) 7500.
- [29] D. Qu, M. Zheng, P. Du, Y. Zhou, L. Zhang, D. Li, H. Tan, Z. Zhao, Z. Xie, Z. Sun, *Nanoscale* 5 (2013) 12272.
- [30] H. Jin, H. Huang, Y. He, X. Feng, S. Wang, L. Dai, J. Wang, *J. Am. Chem. Soc.* 137 (2015) 7588.
- [31] M. Mazloum-Ardakani, A. Khoshroo, L. Hosseinzadeh, *Sensors Actuators B Chem.* 214 (2015)

- 132.
- [32] L. Tang, R. Ji, X. Li, G. Bai, C.P. Liu, J. Hao, J. Lin, H. Jiang, K.S. Teng, Z. Yang, ACS Nano 8 (2014) 6312.
 - [33] D. Li, M.B. Müller, S. Gilje, R.B. Kaner, G.G. Wallace, Nat. Nanotechnol. 3 (2008) 101.
 - [34] M. Mazloum-Ardakani, A. Khoshroo, D. Nematollahi, B.-F. Mirjalili, J. Electrochem. Soc. 159 (2012) H912.
 - [35] W. Hu, Y. Dong, L. Wang, Y. Wang, M. Qian, S. Xi, Comb. Chem. High Throughput Screen. (2021).
 - [36] X. Wang, H. Yu, D. Lu, J. Zhang, W. Deng, Sensors Actuators B Chem. 195 (2014) 630.
 - [37] C.-C. Chang, N.-F. Chiu, D.S. Lin, Y. Chu-Su, Y.-H. Liang, C.-W. Lin, Anal. Chem. 82 (2010) 1207.
 - [38] L. Zhang, Y. He, H. Wang, Y. Yuan, R. Yuan, Y. Chai, Biosens. Bioelectron. 74 (2015) 924.
 - [39] X. Zhang, X. Peng, W. Jin, Anal. Chim. Acta 558 (2006) 110.
 - [40] A. Khoshroo, M. Mazloum-Ardakani, M. Forat-Yazdi, Sensors Actuators B Chem. 255 (2018) 580.
 - [41] I.A. Darwish, T.A. Wani, N.Y. Khalil, D.A. Blake, Talanta 97 (2012) 499.
 - [42] Y.M. Park, S.J. Kim, K. Kim, Y.D. Han, S.S. Yang, H.C. Yoon, Sensors Actuators B Chem. 186 (2013) 571.
 - [43] W. Li, R. Yuan, Y. Chai, S. Chen, Biosens. Bioelectron. 25 (2010) 2548.